

Influence of land use on spatial distribution of primary productivity in aquatic environment in the Weihe River Basin, China

ZHANG Haoying¹, LI Nan^{1,2*}, SONG Jinxi^{1,3}, WANG Fei², TANG Bin¹, GUAN Mengdan¹, ZHANG Chaosong¹, ZHANG Yuchen¹

¹ Xi'an Key Laboratory of Environmental Simulation and Ecological Health in the Yellow River Basin, College of Urban and Environmental Sciences, Northwest University, Xi'an 710127, China;

² Shaanxi Key Laboratory of Environmental Monitoring and Forewarning of Trace Pollutants, Shaanxi Environmental Monitoring Center, Xi'an 710054, China;

³ Yellow River Institute of Shaanxi Province, Northwest University, Xi'an 710127, China

Abstract: Increasing concerns regarding aquatic ecological health and eutrophication driven by urbanization and human activities have highlighted the need to understand primary productivity (PP) dynamics in aquatic ecosystems. This study investigated the spatial distribution of PP across the Weihe River Basin, China using inverse distance weighting and analyzed the influence of different land uses and water physical-chemical parameters on PP using Mantel test and Spearman analysis. Significantly spatial heterogeneity in PP concentrations, ranging from 0.458 to 3262.807 mg C/(m²·d), was observed with high-PP sites clustered in the middle-lower reaches dominated by farmland-construction land mosaics. Core drivers included light availability (Secchi depth and sunlight duration) and phytoplankton biomass (chlorophyll-*a* (Chl-*a*)), while water temperature exhibited threshold-dependent effects. Total organic carbon played dual roles, promoting PP concentrations in low-Chl-*a* regions, but suppressing it under high-Chl-*a* regions. Dual-scale buffer analysis (500 and 1000 m buffer zones) revealed PP heterogeneity stemmed from interactive land use configurations, rather than isolated types. Balanced construction land-to-farmland ratio (0.467–2.890) elevated PP concentrations in human-dominated basins (the main stem of the Weihe River and Jinghe River), whereas excessive agricultural homogenization reduced PP likely due to fertilizer saturation and algal self-shading. Ecologically sensitive basins (the Beiluohe River Basin) demonstrated distinct patterns, in which PP concentration was regulated through natural-agricultural synergies. These results deepened the understanding of land use effects on aquatic PP, providing a theoretical basis for optimizing land use strategies to reconcile eutrophication control with ecological productivity in human-stressed basins.

Keywords: chlorophyll-*a*; water physical-chemical parameters; land use proportions; spatial heterogeneity; Mantel test; Spearman analysis; inverse distance weighting

Citation: ZHANG Haoying, LI Nan, SONG Jinxi, WANG Fei, TANG Bin, GUAN Mengdan, ZHANG Chaosong, ZHANG Yuchen. 2025. Influence of land use on spatial distribution of primary productivity in aquatic environment in the Weihe River Basin, China. Journal of Arid Land, 17(3): 304–323. <https://doi.org/10.1007/s40333-025-0095-6>; <https://cstr.cn/32276.14.JAL.02500956>

*Corresponding author: LI Nan (linan0635@nwu.edu.cn)

Received 2024-11-01; revised 2025-02-10; accepted 2025-03-04

© Xinjiang Institute of Ecology and Geography, Chinese Academy of Sciences, Science Press and Springer-Verlag GmbH Germany, part of Springer Nature 2025

1 Introduction

With increasing global pressure on water resources and the growing demand for aquatic ecosystem health assessments, river primary productivity (PP) has garnered increasing attention, especially in the context of major river systems (Ye et al., 2015; Peng et al., 2021; Chinfak et al., 2023; Oleksy et al., 2024). The PP is regarded as a key indicator of nutrient loading and trophic levels and is of great significance for understanding the functioning of river ecosystem and global changes associated with the carbon and nitrogen cycles (Jia et al., 2019; Zhong et al., 2021; Sun et al., 2023). A national scale study documented that the concentration of PP ranged from 0.000 to 1000.000 mg C/(m²·d) in more than half of the lakes and reservoirs in China. However, compared with lakes (Jia et al., 2019; Yu et al., 2022), reservoirs (Pilla and Griffiths, 2023) and marine ecosystems (Kang et al., 2018; Shiromoto et al., 2023), studies on the PP of riverine ecosystems are relatively scarce (Liu et al., 2022). Given the vital role of rivers as connectors between terrestrial and aquatic systems, it is imperative to assess their PP in order to quantify their contributions to ecosystem services, nutrient cycling, and carbon fluxes.

Over the past few decades, significant attention has been devoted to investigating the impact of point sources, including industrial effluents, municipal sewage discharge, aquaculture waste, and landfill leachates, on PP in aquatic environments (Knight, 2021; Akinnawo, 2023). The leakage of herbicides into seawater has been shown to reduce PP concentration by approximately 5.00%–25.00% (Yang et al., 2024). An enhanced level of PP was observed in an engineered river designed to retain wastewater in India compared with a free-flowing river (Sarkar and Kumar, 2024). In contrast, in the Sacramento River and North San Francisco Estuary in the United States, PP was found to be depressed due to wastewater discharge (Parker et al., 2012). In recent years, targeted policies of the Chinese government have significantly reduced point source pollution in major rivers, including the Yellow River (Quan et al., 2022; Liu et al., 2023). Consequently, the fluctuations in river PP have shifted from being driven by point source pollution to being influenced by non-point source pollution, including agricultural runoff, soil erosion, and urban runoff, all of which are closely linked to land use (Zuo et al., 2023; Zhang et al., 2024). Land use directly alters the quantity and quality of runoff entering water bodies, leading to changes in the pollutant loads and nutrient levels within river systems. Mediterranean freshwater could be highly sensitive to land use types within its watersheds, and a high proportion of agricultural and artificial land cover has been demonstrated to enhance total phytoplankton biomass, which is considered to have a close relationship with PP (Katsiapi et al., 2012; Miranda et al., 2014). Beyond land use types, land use proportion, mosaic structure, and fragmentation also play crucial roles in determining runoff patterns and nutrient fluxes (Siqueira et al., 2023; Locke, 2024). Heterogeneous land use mosaics influence water quality through variations in nutrient retention and sediment transport, which in turn regulate PP (Pramanik, 2023). In contrast, forest land and grassland with higher vegetation cover are less likely to contribute to changes in nutrient levels in water bodies because carbon, nitrogen, and phosphorus are more effectively sequestered or adsorbed in the soil (Doubek et al., 2015; Naipal et al., 2018). These variations in biomass and nutrient dynamics, driven by land use composition and spatial patterns, have direct implications for PP in aquatic systems. Therefore, examining the relationship between land use and river PP is essential for managing river ecosystems and mitigating the impact of land use changes on PP.

The levels of PP in aquatic ecosystems are influenced by a variety of physical-chemical and biochemical factors, including nitrogen and phosphorus availability, light duration, temperature, and pH. Studies have shown that appropriate levels of nitrogen and phosphorus can enhance PP concentrations, whereas excessive concentrations of nitrogen and phosphorus may lead to its decline (Olson and Jones, 2022; Sun et al., 2022). However, the exact roles of nitrogen and phosphorus in facilitating or constraining PP remain debatable. Additionally, the Secchi depth (SD), which affects light penetration, can influence phytoplankton growth and consequently alter PP levels (Sarkar and Kumar, 2024). Other environmental factors such as temperature and pH also influence the physiological processes of aquatic organisms and contribute to changes in PP levels

(Lee et al., 2015; Choi et al., 2020). Land use within watershed can induce changes in these factors, thereby affecting the necessary conditions for PP. Therefore, understanding the impact of land use on aquatic PP requires a comprehensive analysis of the correlation between land use types and the physical-chemical parameters of aquatic environments.

The Weihe River, the largest tributary of the Yellow River, is a vital river for China's Western Development Strategy. Its basin sustains over 2.2×10^7 people and serves as the primary water source for major urban centers in Northwest China, including Xi'an, Baoji, Weinan, and Xianyang cities (Yan et al., 2023). However, in recent years, the basin has experienced significant alterations in land use patterns driven by rapid urbanization, agricultural expansion, and population growth (Zhang et al., 2022). These transformations have profoundly impacted the basin's hydrological processes and ecological conditions, resulting in elevated ecological risks and degraded aquatic ecosystems. (Zhao et al., 2016; Zhang et al., 2021). Particularly concerning is the basin's vulnerability to climate change, exacerbated by its semi-arid climate and high dependence on water resources for agricultural and urban use. This unique combination of environmental stressors makes the Weihe River Basin an ideal study area for investigating the complex interactions between land use changes and PP.

The spatial distribution of PP was investigated across the Weihe River Basin, including the region surrounding its main stem and two major tributaries, the Jinghe River and Beiluohe River. The objectives of this study are: (1) to explore the relationship between spatial distribution of PP and land use types in the Weihe River Basin; (2) to examine the effects of water physical-chemical parameters on PP through Spearman analysis; and (3) to analyze how land use influences spatial distribution of PP based on variations in water physical-chemical parameters through Mantel test. These findings provide insights into the relationship between land use and PP concentrations in the Weihe River Basin, enhancing our understanding of the synergistic effects among watershed land use types, water environmental factors, and PP concentrations in aquatic ecosystems.

2 Materials and methods

2.1 Study area and sampling

The Weihe River Basin ($33^{\circ}50' - 37^{\circ}18'N$, $104^{\circ}00' - 110^{\circ}20'E$) spans Gansu Province, Ningxia Hui Autonomous Region, and Shaanxi Province, and covers an area of $13.5 \times 10^5 \text{ km}^2$ (Lü et al., 2024). Located in the arid and semi-arid areas of Northwest China, the basin is characterized by a temperate continental monsoon climate. The annual precipitation ranges from 500 to 700 mm, with average temperatures varying between 7.80°C and 13.50°C (Xu et al., 2022; Wu et al., 2023). The region features a diverse topography, with the Loess Plateau in the north and the Qinling Mountains in the south. The elevation gradient decreases from west to east, forming the main water systems of the Weihe, Jinghe, and Beiluohe rivers (Chang et al., 2024). This region is rich in diverse vegetation resources including deciduous broad-leaved forests and grasslands. It serves as a critical strategic hub for industrial, agricultural, energy, and economic development in Northwest China as well as a major transportation center (Zhang et al., 2022). The study area included 13 sample sites (W1–W13) along the main stem of the Weihe River, 7 sample sites (J1–J7) in the Jinghe River, and 9 sample sites (B1–B9) in the Beiluohe River (Fig. 1). Sampling was conducted in April and May 2023 in the Weihe River Basin, which is the largest tributary of the Yellow River, China. We selected a total of 29 sample sites along the main stem and the two major tributaries based on geomorphic units, environmental conditions, and established sampling protocols.

2.2 Chemicals and reagents

Acetone ($\text{C}_3\text{H}_6\text{O}$), sulfuric acid (H_2SO_4), hydrochloric acid (HCl), potassium nitrate (KNO_3), and trichloromethane (CHCl_3) were purchased from Sinopharm Chemical Reagent Co., Ltd., (Shanghai, China). Analytical grade alkaline potassium persulfate ($\text{K}_2\text{S}_2\text{O}_8$) was obtained from Sigma-Aldrich (St. Louis, USA). Ascorbic acid ($\text{C}_6\text{H}_8\text{O}_6$), ammonium molybdate ($(\text{NH}_4)_2\text{MoO}_4$),

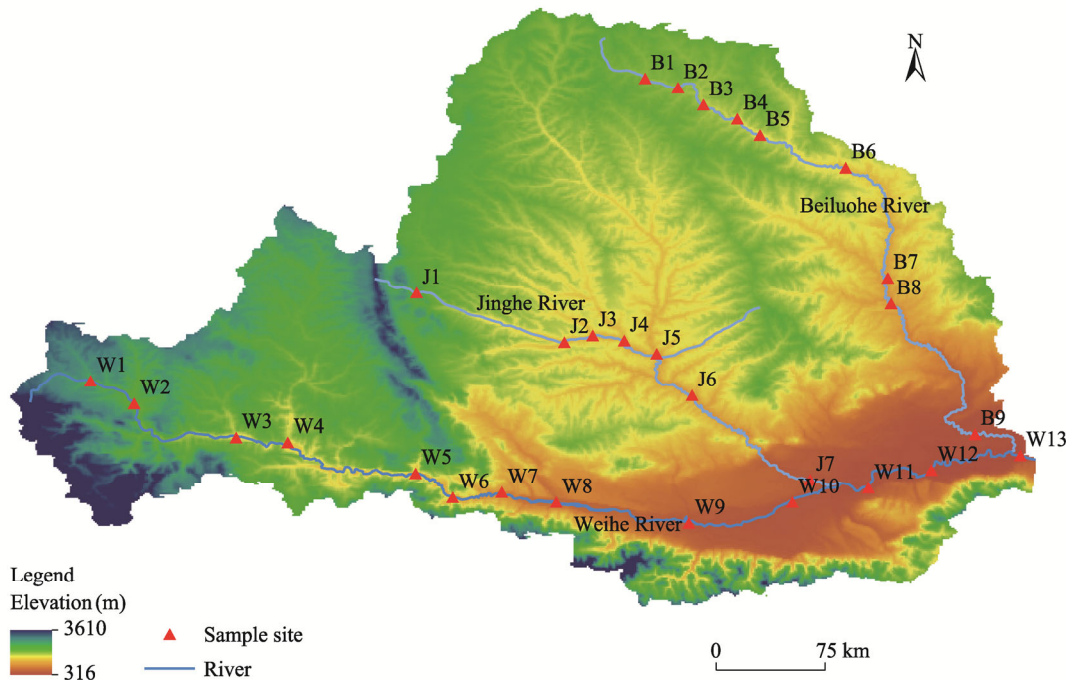


Fig. 1 Overview of study area and the positions of sample sites. The image is sourced from the Data Center for Resources and Environmental Sciences of the Chinese Academy of Sciences (<http://www.resdc.cn>).

potassium antimony tartrate ($C_8H_4K_2O_{12}Sb_2$), and potassium dihydrogen phosphate (KH_2PO_4) were obtained from Tianjin Tianli Chemical Reagent Co., Ltd., Tianjin, China. Ultrapure water (18.2 $M\Omega\cdot cm$) was prepared with a Milli-Q water purification system (IQ7000, Merck Group, Darmstadt, Germany).

2.3 Sample analysis

We measured basic water physical-chemical parameters, including SD, dissolved oxygen (DO), pH, water temperature (WT), sunlight duration (SUN), total nitrogen (TN), total phosphorus (TP), and total organic carbon (TOC) to provide a comprehensive water quality framework of the major physical, chemical, and nutritional characteristics. The SD and SUN are critical for light availability, which can directly influence PP (Harvey et al., 2019). The DO, pH, and WT are fundamental indicators of water quality and ecosystem health (Haddout et al., 2022; Du et al., 2024). And TN, TP, and TOC are key nutrients that drive phytoplankton growth and biogeochemical cycling (Isles et al., 2021). Additionally, these parameters are widely used in water quality assessments due to their sensitivity to anthropogenic activities, such as agricultural runoff, industrial discharge, and urbanization, which are prevalent in the Weihe River Basin (Ren et al., 2021). The DO, pH, and WT were measured onsite using a HACH portable multiparameter tester (HQ40d, Hach Company, Loveland, USA). The SD was measured onsite using a Secchi disk. The SUN was obtained from the weather forecast for the sampling location on the sampling day. Water samples were collected 50 cm below the surface. A 300 mL of water sample was filtered onsite with a 0.45- μm acetate membrane and the membranes were stored in a sterile centrifuge tube at 0.00°C–4.00°C without light for chlorophyll-*a* (Chl-*a*) detection. The remaining water samples were stored in pre-cleaned polyethylene bottles. All samples were immediately transported to the laboratory, stored in 0.00°C–4.00°C without light, and analyzed within 72 h.

We measured Chl-*a* level in the laboratory according to the national standard methods for examining water and wastewater in China (State Environmental Protection Administration of the People's Republic of China, 2002). The membrane samples were dissolved in 10 mL of 90.00% propanol solution, statically extracted in the dark for 24 h, and centrifuged for 10 min at 3500

r/min. The supernatant was placed in a 10-mm quartz cuvette for absorbance measurements at 630, 645, 663, and 750 nm using a Thermo spectrophotometer (AQ8000, Thermo Fisher Scientific, Waltham, USA). Water samples were filtered by 0.45 μm aqueous fiber membrane for the analysis of TN, TP, and TOC. The TOC was determined using an elementar TOC analyzer (vario TOC select, Elementar Analysensysteme GmbH, Langenselbold, Germany). The TP and TN were analyzed using ammonium molybdate spectrophotometric method (Ministry of Ecology and Environment of the People's Republic of China, 1990) and alkaline potassium persulfate digestion UV spectrophotometric method (Ministry of Ecology and Environment of the People's Republic of China, 2012), respectively. Additionally, the ratio of total nitrogen to total phosphorus (TN/TP ratio) was calculated using measured concentrations of TN and TP to better evaluate nutrient limitations.

2.4 Evaluation of PP

After blank correction, we calculated concentration of Chl- a according to the water and wastewater monitoring and analysis method using the following formula (State Environmental Protection Administration of the People's Republic of China, 2002).

$$C_a = \frac{[11.64 \times (D_{665} - D_{750}) - 2.16 \times (D_{645} - D_{750}) + 0.10 \times (D_{630} - D_{750})] \times V_1}{V \times \delta}, \quad (1)$$

where C_a is the concentration of Chl- a in water body (mg/L); V is the volume of the filtered water sample (L); D_{630} , D_{645} , D_{663} , and D_{750} are the absorbance of 630, 645, 663, and 750 nm, respectively; V_1 is the volume after volumetric adjustment (mL); and δ is the optical length of the cuvette (cm).

The PP was calculated using the simplified formula proposed by Cadée (1975).

$$P = \frac{P_s \times E \times D}{2}, \quad (2)$$

where P is the daily primary productivity of the sample site (mg C/(m²·d)); E is the depth of the euphotic layer (m), which is 3.05 times Secchi depth; D is the sunlight exposure (h/d); and P_s is the potential productivity of phytoplankton in surface water (mg C/(m²·d)), which can be calculated by the content of Chl- a in surface water as follows (Wu et al., 2022):

$$P_s = C_a \times Q, \quad (3)$$

where Q is the assimilation coefficient, which is usually 3.70 mg/(mg·h), according to the empirical value proposed by Cadée (1975).

2.5 Land use types in the Weihe River Basin

We obtained the land use data at 30 m resolution from the Resources and Environmental Scientific Data Platform, Chinese Academy of Sciences (<http://www.resdc.cn>). Land use types were categorized into six classes: farmland, forest land, grassland, construction land, water body, and unutilized land. We extracted concentric buffer zones of 500 and 1000 m around sample sites to systematically quantify the spatial distribution and proportional area of land use types under varying scales using ArcGIS v.10.8 (Environmental Systems Research Institute Inc. (ESRI), Redlands, USA) (Lu et al., 2023). Then, we calculated the proportion of each land use type in the catchment to determine the distribution of land use types across the Weihe River Basin.

2.6 Statistical analysis and quality control

We used inverse distance weighting to estimate the spatial distribution of PP throughout the Weihe River Basin. A spatial analyst extracted the data from the inverted region. We compared the extracted values with the measured values to evaluate accuracy. The results revealed a variance of 0.048 and a standard deviation of 0.220, demonstrating the extracted values exhibit high reliability and stability in estimating spatial distribution of PP across the Weihe River Basin. We collected and analyzed all samples in two parallel sets to provide an average coefficient of variation below 10.00%. The relative standard deviations of 89.66% samples ranged from 0.05%

to 18.15%, while the remaining 10.34% showed higher variability, with relative standard deviation values exceeding 20.00%. This elevated variability in a small subset of samples was likely attributable to localized environmental disturbances, such as riverbed instability and turbidity fluctuations. Despite these anomalies, statistical validation confirmed that the core trends and patterns identified in the study remained robust, as 89.66% of the dataset exhibited acceptable precision.

2.6.1 Normalization of Chl-*a* and PP

To enhance data comparability, we normalized Chl-*a* and PP data to effectively observe differences among sampling sites. The min-max normalization was used for the data of Chl-*a* and log-normalization was used for the data of PP. We selected each method based on the distribution and characteristics of the data. The min-max normalization rescales the data to a fixed range, typically [0, 1], by transforming each value relative to the minimum and maximum values of the dataset (Sinsomboonthong, 2022). The log-normalization compresses the scale of large values while maintaining the relative differences between observations (Booeshaghi and Pachter, 2021).

2.6.2 Spearman analysis

Spearman analysis is suitable for assessing the strength and direction of associations between variables without assuming linearity or normality in the data distribution (MacFarland and Yates, 2016). In this study, we conducted Spearman analysis to analysis the relationship between PP and water physical-chemical parameters using OriginPro v.2023 (OriginLab Corporation, Northampton, Massachusetts, USA). The Spearman's rank correlation coefficient can be calculated using the formula:

$$\rho = 1 - \frac{6 \sum d_i^2}{n(n^2 - 1)}, \quad (4)$$

where ρ is the Spearman's rank correlation coefficient; d_i is the difference between the ranks of corresponding observations for the two variables; and n is the sample size. The coefficient ρ ranges from -1.00 to 1.00, where values close to 1.00 indicate a strong positive relationship, values close to -1.00 indicate a strong negative relationship, and values near 0.00 suggest no relationship. The significance of the correlation was determined using Spearman's *P* values, with thresholds setting as: obviously significant ($P < 0.01$), significant ($P < 0.05$), or not significant ($P > 0.05$) (Helsel et al., 2020).

2.6.3 Mantel test

We adopted Mantel test to explore the relationship between land use types and water physical-chemical parameters. Mantel test assesses the relationship between two distance matrices: one representing land use type and the other representing water physical-chemical parameter, using a permutation-based approach. The analysis was conducted using the "ggcor" package in R software (RStudio, Boston, USA), with Spearman analysis being applied to measure the monotonic relationship. We classified the strength of the correlation based on Mantel's *r* values as follows: weak ($r < 0.2$), moderate ($0.2 \leq r \leq 0.4$), or strong ($r > 0.4$). The significance of the correlation was determined using Mantel's *P* values, with thresholds setting as: obviously significant ($P < 0.01$), significant ($0.01 \leq P \leq 0.05$), or not significant ($P > 0.05$). These classifications follow established guidelines for interpreting Mantel test results (Harmon and Glor, 2010).

3 Results

3.1 Spatial distribution of Chl-*a* and PP

The Chl-*a* was detected at all 29 sample sites during all sampling events. The normalized Chl-*a* concentration and PP at the three sampled rivers are shown in Figure 2. The main stem of the Weihe River exhibited the highest average concentrations of Chl-*a* and PP, followed by the Jinghe tributary (Table 1). The spatial distribution of PP in the whole basin is shown in Figure 3, exhibiting an increasing trend from the upstream to the downstream areas in the whole Weihe River Basin.

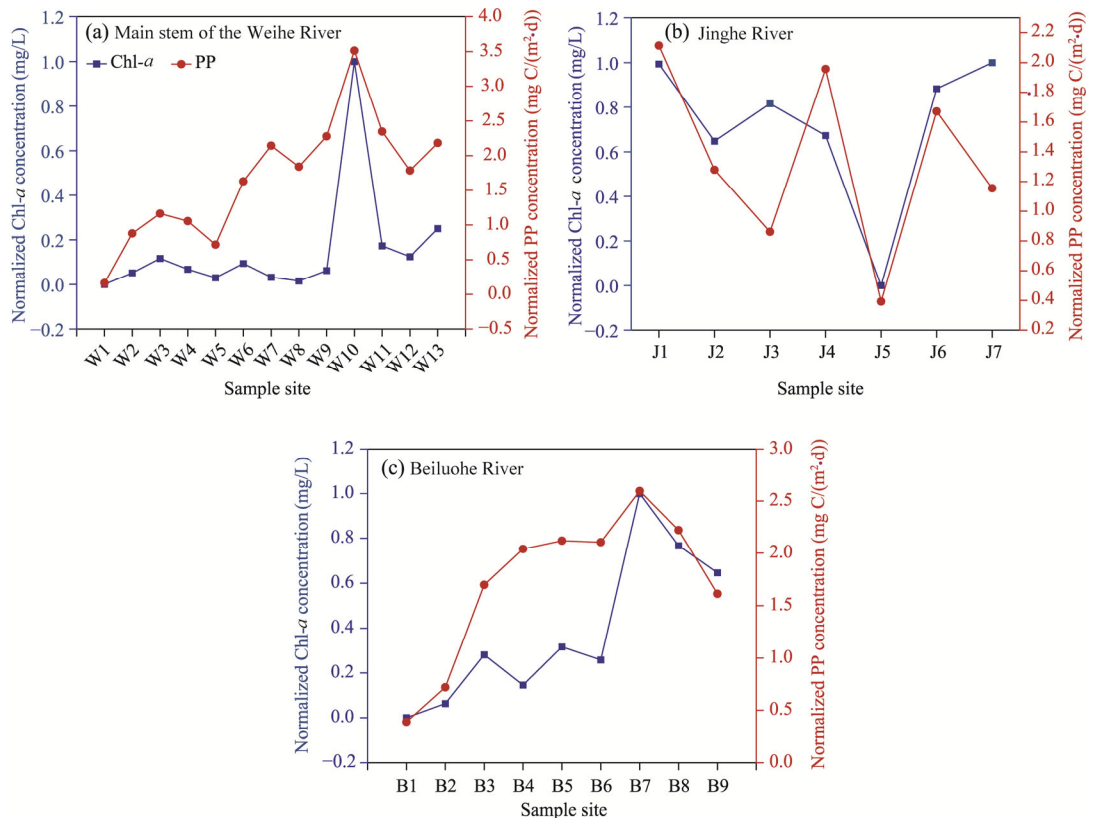


Fig. 2 Normalized concentrations of chlorophyll-*a* (Chl-*a*) and primary productivity (PP) of each sample site in the Weihe River Basin. (a), main stem of the Weihe River; (b), Jinghe River; (c), Beiluohhe River.

Table 1 Concentrations of chlorophyll-*a* (Chl-*a*) and primary productivity (PP) of three rivers in the Weihe River Basin

River	Concentration of Chl- <i>a</i> (mg/L)				Concentration of PP (mg C/(m ² ·d))			
	Maximum	Minimum	Median	Mean	Maximum	Minimum	Median	Mean
Main stem of the Weihe River (<i>n</i> =13)	72.920	0.615	5.533	11.853	3262.807	0.458	60.105	320.591
Jinghe River (<i>n</i> =7)	4.838	0.620	4.060	3.642	129.266	1.469	18.020	43.418
Beiluohhe River (<i>n</i> =9)	10.133	0.072	2.901	3.959	393.767	1.442	108.466	113.186

Note: *n* is the number of sample sites.

The range of Chl-*a* concentration and PP concentration in the main stem of the Weihe River was 0.615–72.920 mg/L and 0.458–3262.807 mg C/(m²·d), respectively. In the main stem of the Weihe River, the maximum levels of Chl-*a* concentration and PP concentration observed at site W10 were over 1000 times higher than those observed at the minimum site (site W1). Site W10 is located within a landscape and the surrounding land is predominantly urbanized, comprising factories, and residential development. Construction land likely contributes to increased nutrient loading, creating favorable conditions for phytoplankton growth, and leading to elevated levels of PP. Except for site W10, the Chl-*a* concentrations at all sites were less than 18.748 mg/L.

In the Jinghe River, the concentration of Chl-*a* at site J5 was the lowest at 0.620 mg/L. At other sites, the concentration of Chl-*a* ranged from 3.335 to 4.838 mg/L. The median concentration of Chl-*a* in the Jinghe River was 4.060 mg/L, which was slightly lower than that in the main stem of Weihe River. The PP concentrations in the Jinghe River ranged from 1.469 to 129.266 mg C/(m²·d), with a mean and median of 43.418 and 18.020 mg C/(m²·d), respectively.

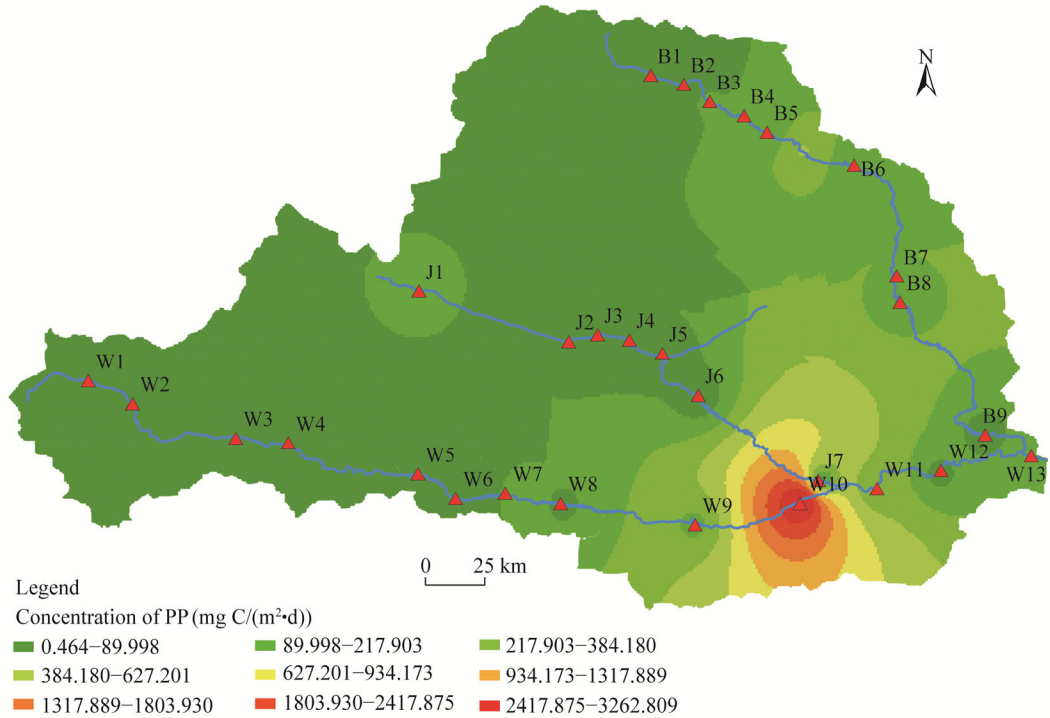


Fig. 3 Spatial distribution of PP in the Weihe River Basin in April and May 2023

Corresponding to the Chl-*a* concentration, PP concentration at site J5 was also minimal in the Jinghe River. Site J5 is situated in the middle section of the Jinghe River and is characterized by steep cliffs along the riverbanks and predominantly undeveloped surrounding land. The riverbed is composed of red sandstone with an exposed bedrock, resulting in low nutrient availability. These conditions are unfavorable for phytoplankton growth, leading to relatively low levels of PP. However, the highest concentration of Chl-*a* at site J7 resulted in low levels of PP. The high Chl-*a* concentration at site J7 is likely attributed to the influx of terrestrial nutrients due to severe soil erosion, promoting phytoplankton growth. However, the low PP levels during the sampling period may result from high turbidity caused by rainfall, which limits light availability and photosynthetic activity.

The levels of Chl-*a* and PP in the Beiluhe River ranged from 0.072 to 10.133 mg/L and from 1.442 to 393.767 mg C/(m²·d), respectively. Both Chl-*a* and PP showed increasing trends, with some fluctuations, along the Beiluhe River from upstream to downstream. In summary, the main stem of the Weihe River exhibited the highest PP, while the Jinghe River showed the lowest value across the basin. Spatially, both PP and Chl-*a* concentrations followed a consistent longitudinal gradient, demonstrating a synchronous increasing trend from upstream to downstream regions.

3.2 Relationship between water physical-chemical parameters and PP

The statistical analysis results for the physical-chemical parameters of water (i.e., SUN, SD, pH, WT, DO, TOC, TN, TP, and TN/TP ratio) are listed in Table S1. The average SUN was 13.63 h/d, and the variation during the sampling period did not exceed 3.39%. The WT exhibited an upward trend over the sampling period, with a variation rate exceeding 24.11%. The pH of the entire Weihe River Basin remained at approximately 8.50. The TP was only 0.457 mg/L in the main stem and almost 0.013 mg/L for both tributaries. The average TOC concentration in the main stem of the Weihe River was almost 2–3 times higher than those in the two tributaries. The highest average DO, TN, and SD values were recorded in the Beiluhe River.

Spearman analysis was conducted to evaluate the relationships between water physical-chemical parameters and PP in the Weihe River Basin (Fig. 4). In the main stem of the

Weihe River, PP showed significant positive correlations with SD ($P<0.01$, $\rho=0.93$), WT ($P<0.01$, $\rho=0.88$), and Chl-*a* ($P<0.05$, $\rho=0.58$), and had a weak positive correlation with pH, DO, and TN/TP ratio. The PP also exhibited significant negative correlations with SUN ($P<0.01$, $\rho=-0.70$) and TOC ($P<0.01$, $\rho=-0.84$), and weakly negative relationships with TN and TP. In the Jinghe River, PP was significantly positively correlated with SD ($P<0.01$, $\rho=0.96$), DO ($P<0.01$, $\rho=0.89$), and pH ($P<0.05$, $\rho=0.85$), and weakly positively correlated with TOC, TN/TP ratio, and Chl-*a*. Meanwhile, it was weakly negatively correlated with SUN, WT, TN, and TP. In the Beiluohe River, PP exhibited significantly positive correlations with TP ($P<0.05$, $\rho=0.72$) and Chl-*a* ($P<0.05$, $\rho=0.78$), and exhibited weakly positive relationships with pH, TOC, SD, and WT. Therefore, the physical-chemical parameters in the Weihe River Basin exhibited pronounced spatial heterogeneity in their relationships with PP. Factors such as SUN, SD, and pH showed consistent influence across the three rivers, while the effects of WT, TP, and TOC displayed divergent roles. These spatially varying interactions, coupled with the synergistic effects of nutrient stoichiometry (TN/TP ratio) and algal biomass (Chl-*a*), indicated that PP variability in the basin was governed by region-specific combinations of physical, chemical, and biological drivers.

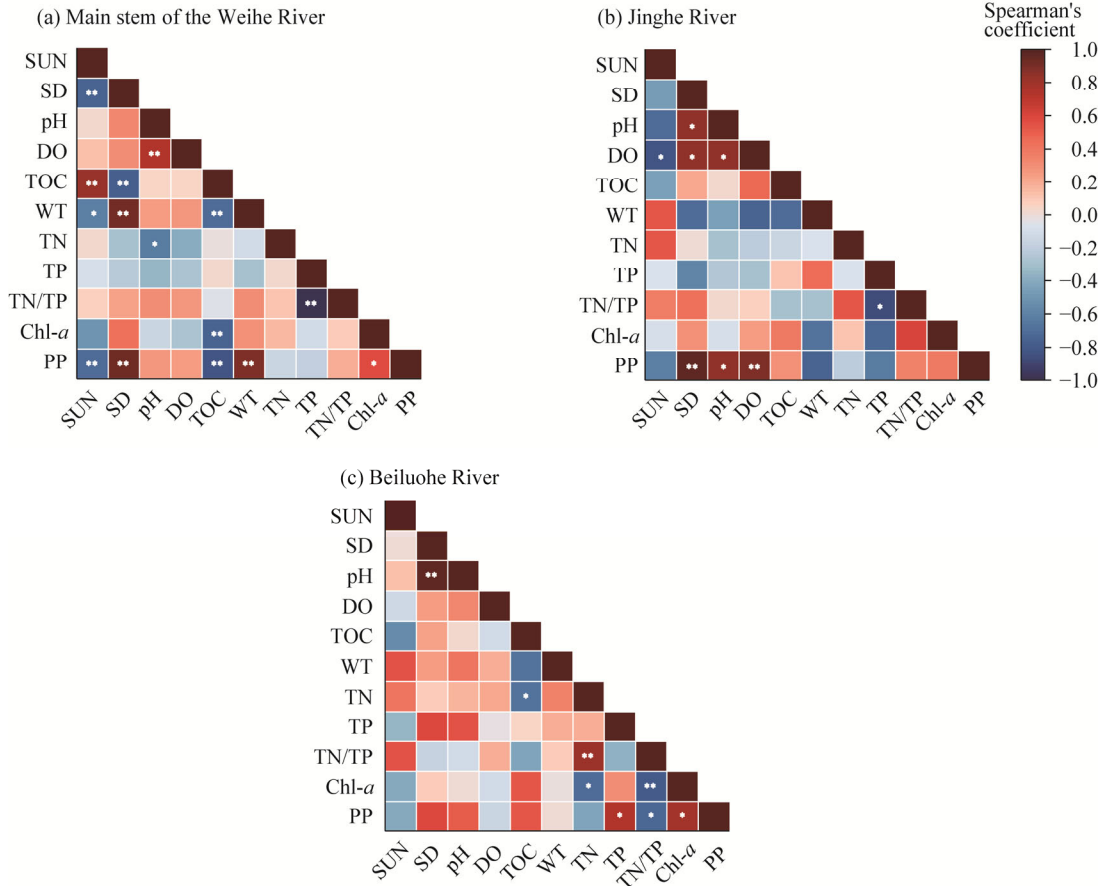


Fig. 4 Spearman analysis of relationships between water physical-chemical parameters and PP in the Weihe River Basin. (a), main stem of the Weihe River; (b), Jinghe River; (c), Beiluohe River. SUN, sunlight duration; SD, Secchi depth; WT, water temperature; DO, dissolved oxygen; TOC, total organic carbon; TN, total nitrogen; TP, total phosphorus; TN/TP, ratio of total nitrogen to total phosphorus. *, $P<0.05$ level; **, $P<0.01$ level.

3.3 Relationship between land use and PP

3.3.1 Distribution of land use types in the Weihe River Basin

The distribution of land use types in the Weihe River Basin is shown in Figure 5. The region

around the main stem of the Weihe River featured the largest proportion of farmland, covering 31.18%, followed by forest land, which accounted for 24.37% (Fig. S1). Farmland, forest land, and grassland collectively accounted for 73.33% of the region of the main stem of the Weihe River. In contrast, grassland was the predominant land use type in regions around both the Jinghe and Beiluohhe rivers, comprising 44.60% and 35.83% of their total areas, respectively. Farmland and forest land were the second largest land use types in the regions around the Jinghe and Beiluohhe rivers, respectively. Farmland, forest land, and grassland accounted for over 90.53% of all the land use types in regions around these two tributary basins. The main stem region had the largest proportion of construction land (15.98 %), whereas the proportion of construction land in regions around the two tributaries was below 2.94%. Construction land was primarily concentrated downstream of the main stem and in the confluence regions of the main stem and its tributaries. No unutilized land was observed in the study area, due to intensive human activities and comprehensive land development in the Weihe River Basin.

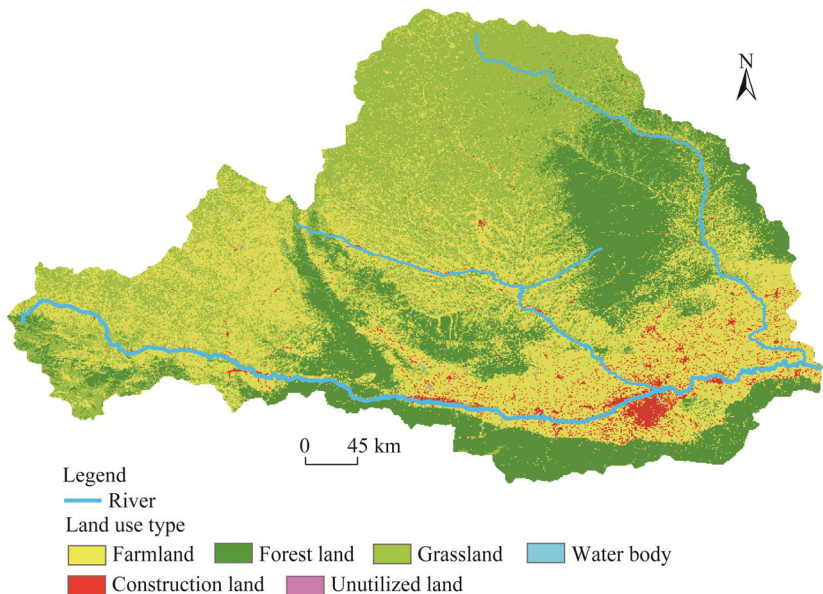


Fig. 5 Distribution of land use types in the Weihe River Basin

3.3.2 Land cover proportions and PP

The spatial distribution of PP in the Weihe River Basin was predominantly influenced by the compositional ratios of land use types within 500 and 1000 m buffer zones, rather than individual land use types (Fig. 6). This suggested that synergistic interactions between land use types drive PP variations. In the main stem of the Weihe River, high-PP sites (W9, W10, and W11) exhibited a synergistic dominance of farmland and construction land (>71.75% coverage), with construction land-to-farmland ratio decreasing from 0.542–2.890 (500 m buffer zones) to 0.467–2.104 (1000 m buffer zones), suggesting that construction land expansion within closer proximity strongly elevated PP levels. Conversely, low-PP sites (W1, W2, and W5) were linked to monocultural landscapes dominated by grassland or farmland (>81.50% coverage), particularly in 1000 m buffer zones with extreme farmland-to-grassland ratio (1.816–70.177), indicating PP suppression under reduced land use diversity. Similar patterns emerged in the Jinghe River, where high-PP sites, including J1 and J4, showed balanced land use mosaics, with a construction land-to-farmland ratio of approximately 2.136 within 500 m buffer zones. In contrast, PP levels decreased in areas dominated by agricultural homogenization (J3 and J5), where the construction land-to-farmland ratio ranged from 0.000 to 0.628, further highlighting the positive association between higher construction land ratios and elevated PP levels. Notably, the Beiluohhe River

exhibited region-specific drivers of PP variability. Higher-PP sites (B6, B7, and B8) were associated with forest land or grassland in 500 m buffer zones (>93.01% coverage; farmland-to-grassland ratio: 0.000–0.078), whereas within 1000 m buffer zones, these sites displayed more heterogeneous land cover, characterized by a higher diversity of land use types and an increased farmland proportion (farmland-to-grassland ratio: 0.373–0.465). This transition suggested that moderate farmland expansion within mixed land use configurations facilitated elevated PP levels, likely through enhanced resource availability and synergistic interactions between agricultural and natural vegetation. In contrast, low-PP sites (B1, B2, and B9) were linked to homogeneous landscapes dominated by more than 85.47% grassland or farmland, with minimal land use diversity (farmland-to-grassland ratio: 0.044–0.160), where limited ecological complexity constrained productivity. These contrasts highlighted dual mechanisms: construction land enhanced PP in human-dominated basins (the main stem of the Weihe River and Jinghe River) through nutrient inputs, while in ecologically sensitive areas (the Beiluohe River), PP relied on natural vegetation-agriculture synergies. Thus, spatially optimized land use combinations, rather than isolated types, critically govern PP dynamics across heterogeneous landscapes.

3.4 Effect of land use types on water physical-chemical parameters

Mantel test revealed the relationships between land use types and water physical-chemical parameters in the main stem of the Weihe, Jinghe, and Beiluohe rivers (Fig. 7). Within the 500 and 1000 m buffer zones around the sample sites, the correlation between land use types and water physical-chemical parameters varied with spatial scale, highlighting the spatial heterogeneity of land use impacts on aquatic ecosystems. Notably, unutilized land was not extracted in the buffer zones of the main stem of the Weihe River, while both unutilized land and water body were absent in the buffer zones of the Jinghe and Beiluohe rivers. In the main stem of the Weihe River, construction land in the 500 m buffer zones showed a significant positive correlation with TN/TP ratio ($P<0.01$). And water body in the same zones was positively correlated with SUN ($P<0.05$). In the 1000 m buffer zones, farmland was significantly positively correlated with DO and SD ($P<0.05$). Grassland exhibited highly significant positive correlations with SUN, WT, and TOC ($P<0.01$). Water body was also positively correlated with SUN ($P<0.01$) and WT ($P<0.05$). In the Jinghe River, grassland in the 500 m buffer zones was positively correlated with pH ($P<0.01$). Farmland in the 1000 m buffer zones showed a highly significant positive correlation with DO ($P<0.01$). In the Beiluohe River, no significant correlations were observed between land use types and water physical-chemical parameters in either the 500 or 1000 m buffer zones. Thus, the spatial heterogeneity of land use impacted aquatic ecosystems, demonstrating that different land use types differentially affected the water environment through nutrient inputs, dissolved oxygen regulation, and organic matter cycling.

4 Discussion

4.1 Effects of water physical-chemical parameters on PP

4.1.1 Main drivers

The observed correlations between PP and water physical-chemical parameters across the Weihe River Basin highlighted the central role of light availability (SD and SUN) and phytoplankton biomass (Chl-*a*) in regulating PP levels (Fig. 4). Strong positive correlations between PP and Chl-*a* in the main stem of the Weihe River and the Beiluohe River confirmed Chl-*a* as a direct proxy for phytoplankton-driven PP (Yamaguchi et al., 2020). Concurrently, SD and SUN modulated light penetration, with higher SD and reduced SUN enhancing PP levels by improving photosynthetic efficiency (Dokulil and Qian, 2021). Notably, the dominance of Chl-*a* over SUN in driving PP variability (e.g., the main stem of the Weihe River) suggested that phytoplankton biomass compensated for moderate light limitation through adaptive growth strategies, aligning with findings from global lake studies (Xie et al., 2024).

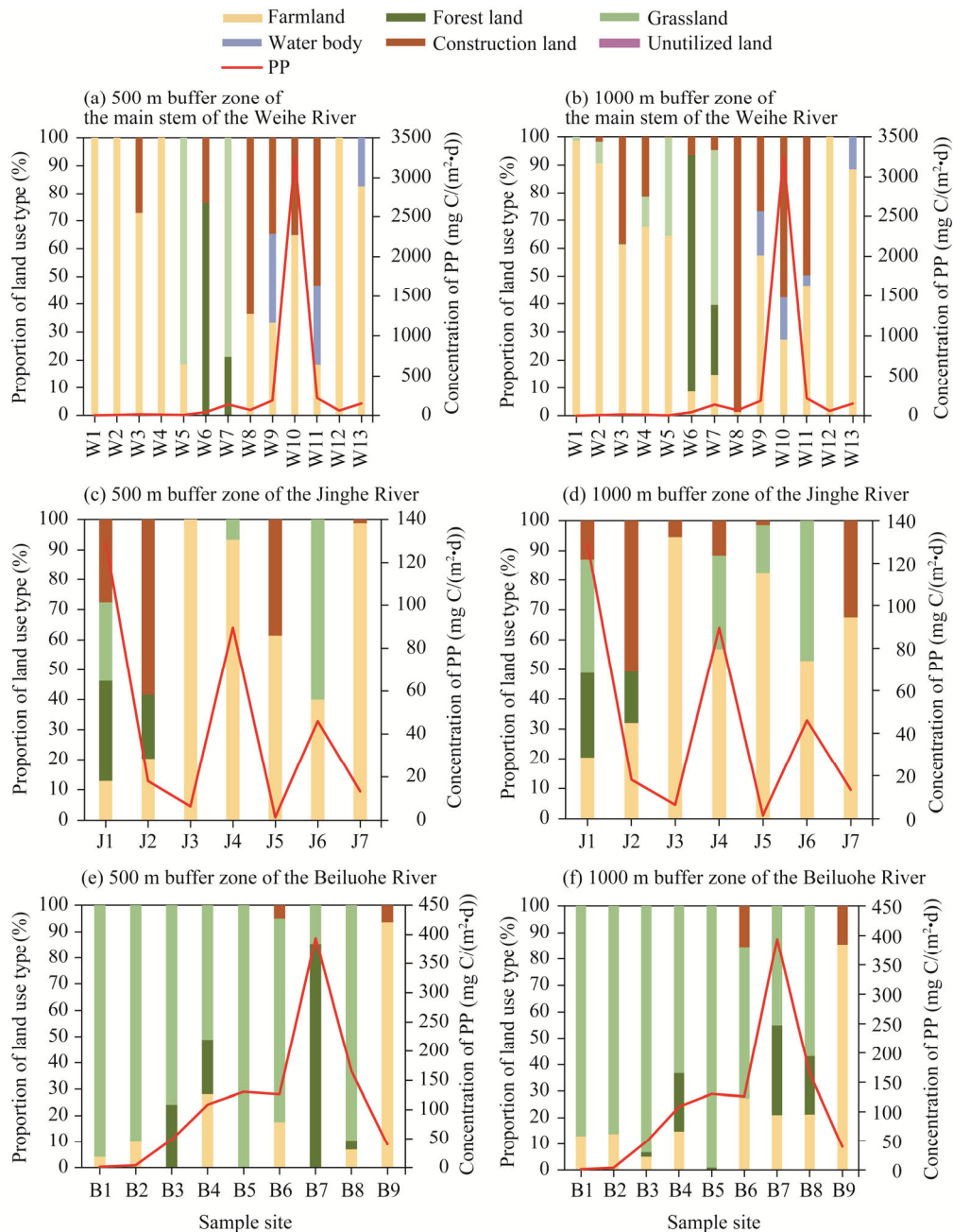


Fig. 6 Relationship between area proportion of land use types and PP in the 500 (a, c, and e) and 1000 (b, d, and f) m buffer zones in the Weihe River Basin

4.1.2 WT and pH

The WT exhibited contrasting effects: positive correlations in the main stem of the Weihe River and the Beiluohe River versus a weak negative trend in the Jinghe River. This discrepancy likely reflected thermal thresholds for phytoplankton metabolism. About 85.71% of sample sites in the Jinghe River predominantly situated in environments of $WT < 20.00^{\circ}\text{C}$ (suboptimal for growth), whereas 61.54% of sample sites with higher WT ($> 20.00^{\circ}\text{C}$) in the main stem of the Weihe River had higher PP levels, being consistent with temperature-dependent productivity thresholds (Bai et al., 2006; Zhao et al., 2019). Similarly, stable pH (pH variation < 0.50) created a neutral microenvironment conducive to phytoplankton activity, minimizing pH-driven constraints.

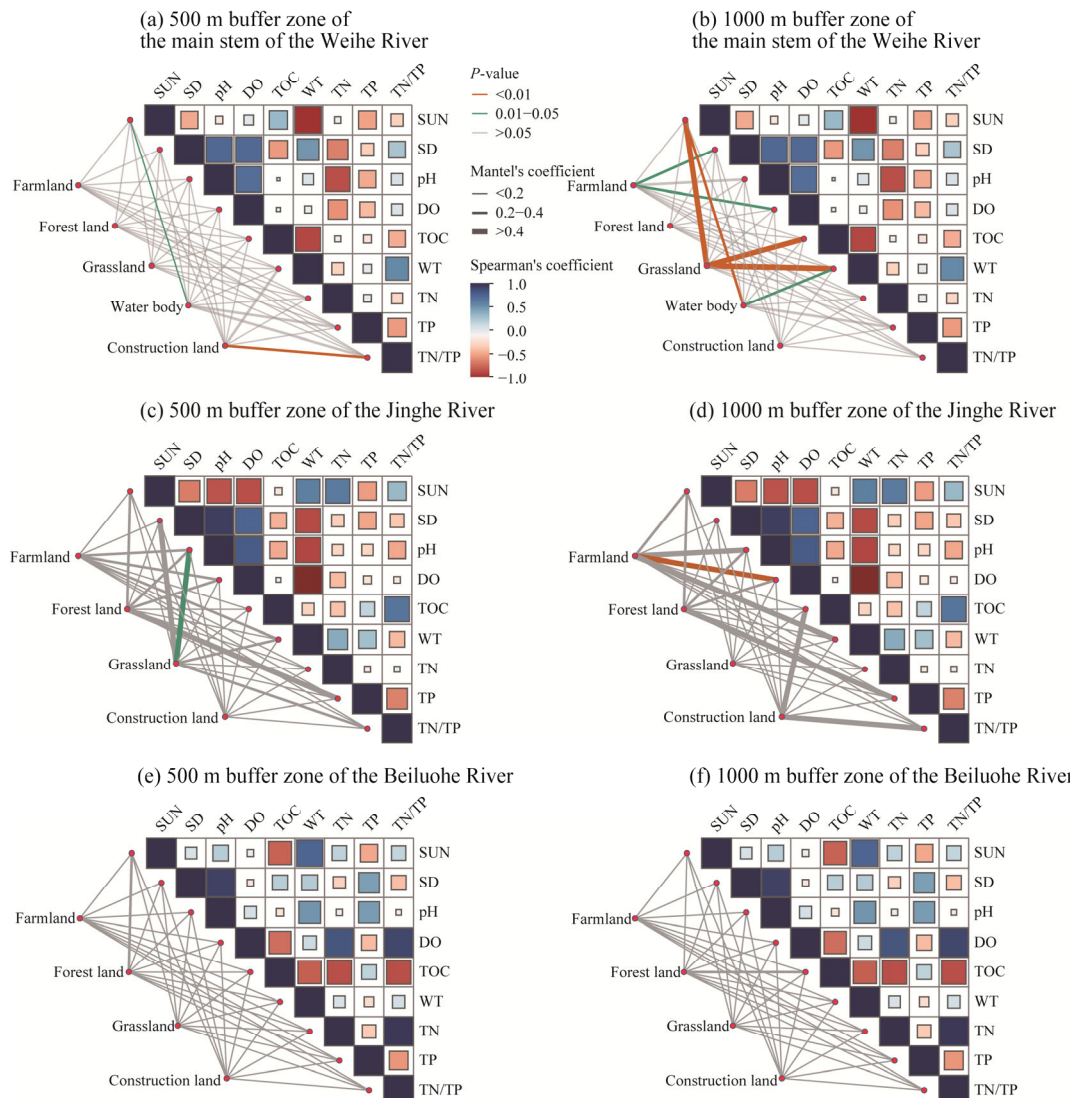


Fig. 7 Mantel test between water physical-chemical parameters and land use types in the 500 (a, c, and e) and 1000 (b, d, and f) m buffer zones in the Weihe River Basin

4.1.3 Organic and nutrients dynamics

The dual role of TOC exemplified context-dependent nutrient interactions. While TOC positively correlated with PP in the Jinghe and Beiluohe rivers, it showed a significantly negative relationship in the main stem of the Weihe River. This inversion might stem from Chl-*a*-mediated resource competition. Elevated phytoplankton biomass, particularly the higher Chl-*a* levels in the main stem compared with two tributaries, likely increased TOC consumption. This pattern resembled marine systems, where high Chl-*a* concentrations reduced dissolved organic carbon (Li et al., 2012).

The PP responded variably to TN/TP ratios across the basin. In the main stem of the Weihe River and Jinghe River, balanced ratios synergistically enhanced PP levels, which is consistent with nutrient stoichiometry theory as proposed by Elser et al. (2009). However, the Beiluohe River, impacted by anthropogenic pollution and ecological fragility (Li et al., 2024), displayed severe imbalance of TN/TP ratios, leading to TP limitation ($P<0.05, \rho=0.72$) that suppressed both phytoplankton growth and dissolved oxygen production. This phenomenon aligned with eutrophic areas where skewed TN/TP ratios disrupt aquatic productivity (Bratt et al., 2020).

4.1.4 DO feedback

The positive DO-PP correlation in the Jinghe River reflected a photosynthesis-respiration feedback mechanism, whereby phytoplankton-derived oxygen elevated DO, subsequently enhancing metabolic rates and amplifying PP, as observed in aquatic ecosystems (Cui et al., 2021). However, TP limitation in the Beiluohe River disrupted this feedback loop, resulting in simultaneous declines in both DO and PP. These findings collectively demonstrated that PP was governed by hierarchical controls in the Weihe River Basin, where light-phytoplankton interactions dominated the core dynamics, while auxiliary factors (e.g., nutrients and temperature) exerted context-dependent effects modulated by regional anthropogenic and ecological conditions.

4.2 Influences of land use on PP

Land use types exert controls on aquatic PP by regulating nutrient and contaminant inputs, as well as light availability (Liao et al., 2016; Qu et al., 2022). In the Weihe River Basin, a comparative analysis of land use types and the spatial distribution of PP demonstrated that high-PP sites predominantly clustered in the middle-lower reaches (Fig. 2), where mosaics of intensive farmland and construction land dominated the landscape (Fig. 5). This pattern indicated the synergistic role of anthropogenic land uses in elevating PP levels, as these areas act as primary conduits for nitrogen and phosphorus inputs via agricultural runoff and urban effluents (Katsiapi et al., 2012). Specifically, excess nutrients from fertilizers and wastewater stimulate phytoplankton proliferation, directly enhancing PP levels (Li et al., 2022). In addition, construction land expansion reduces riparian vegetation cover, increasing light penetration and further amplifying productivity—a dual mechanism linking land use intensification to aquatic carbon fixation.

4.2.1 Driving effects of synergistic land use configuration on PP heterogeneity

The establishment of dual-scale buffer zones (500 and 1000 m) enabled a systematic quantification of spatially heterogeneous land use-PP linkages across the Weihe River Basin (Fig. 6). This approach aligns with landscape ecological frameworks emphasizing scale-dependent interactions between terrestrial and aquatic systems (Gove et al., 2001). The results demonstrated that PP in the Weihe River Basin was shaped not by individual land use types in isolation but by the spatial configuration and proportional interactions among them across multi-scale buffer zones. A striking dichotomy emerged between human-dominated basins (the main stem of the Weihe River and Jinghe River) and ecologically preserved systems (the Beiluohe River). In the Weihe and Jinghe rivers, high-PP levels were strongly associated with a balanced mosaic of farmland and construction land (>71.75% combined coverage), where the construction land-to-farmland ratio (0.542–2.890 at 500 m buffer zones; 0.467–2.104 at 1000 m buffer zones) regulated nutrient flux intensity. This observation corroborated Tu's threshold theory, which demonstrated that the contribution of farmland might become statistically insignificant when construction land surpassed more than one-third area coverage (Tu, 2011). Conversely, PP suppression was observed in monocultural landscapes (e.g., W1 and W2 with >81.50% grassland or farmland coverage), where homogeneous land cover reduced material exchange interfaces, thereby limiting allochthonous energy subsidies to aquatic systems.

4.2.2 Dual effects of construction land and farmland intensification on PP regulation

The positive correlation between construction land proximity and PP (e.g., W9–W11 and J1–J4) suggested that infrastructure-driven eutrophication played a significant role in shaping ecosystem dynamics. High impervious surface ratios within 500 m buffer zones likely accelerated nutrient transport via stormwater conduits, thereby overriding nutrient retention mechanisms associated with agricultural land (Bell et al., 2019). However, excessive agricultural homogenization (e.g., J3 and J5 with construction land-to-farmland ratio of 0.000–0.628) was linked to PP suppression, indicating a dual mechanism of fertilizer saturation and light limitation induced by algal blooms. This paradox highlighted the need for threshold-based land use zoning to mitigate eutrophication while maintaining ecosystem productivity (Huang et al., 2024).

4.2.3 Effects of natural-agricultural spatial coupling on PP modulation

Ecologically sensitive basin (the Beiluohe River) exhibited distinct patterns, where PP was regulated by natural-agricultural synergies. High-PP sites (B6–B8) were characterized by a "natural vegetation shield" within the 500 m buffer zone (>93.01% forest land or grassland), which effectively mitigated loess erosion. Meanwhile, the integration of farmland within the 1000 m buffer zones (farmland-to-grassland ratio: 0.373–0.465) provided moderate nutrient subsidies, facilitating a balance between sediment control and productivity enhancement. Conversely, low-PP sites (B1, B2, and B9) suffered from homogeneous land cover (>85.47% grassland or farmland). The porous structure of loess soil reduced the capacity of grassland to intercept nutrients (Phileze, 2010), while homogeneous farmland configurations may lead to pulsed fertilizer inputs, exacerbating algal self-shading effects (Fried et al., 2003). These findings challenged conventional riparian management paradigms, suggesting that ecological conservation on the Loess Plateau must move beyond the "maximal vegetation coverage" approach. Instead, a spatially tiered strategy is essential to maintain a balance between erosion control and sustainable productivity (Zhao et al., 2012).

4.3 Limitations

Due to operational constraints in field logistics, this study focused only on the normal flow period, which may limit the temporal and spatial representativeness of the results. Seasonal variations in hydrological conditions, such as low- and high-flow periods, can significantly influence nutrient transport, light availability, and PP in aquatic ecosystems (Bian et al., 2021). To enhance the robustness of future research, it would be beneficial to extend sampling to multiple seasons, capturing seasonal variations and providing a more comprehensive understanding of PP dynamics in aquatic ecosystems. Additionally, while construction land use implicitly incorporates anthropogenic pressures, direct quantification of specific disturbances (particularly point-source sewage emissions) is lacking. Municipal wastewater inputs alter aquatic ecosystems by introducing exogenous nutrients and labile organic matter, which may override land use-mediated PP responses and exacerbate eutrophication risks (Bonsdorff, 2021; Preisner et al., 2021). To isolate the ecological effects of land use types, subsequent research should integrate pollution source apportionment techniques (e.g., isotopic tracers) to differentiate diffuse versus point-source contributions.

5 Conclusions

This study investigated the spatial distribution of PP in the Weihe River Basin and its relationship with land use and water physical-chemical parameters. The results demonstrated significant spatial heterogeneity in PP, with high-PP regions primarily located in human-dominated basins characterized by farmland-construction land mosaics. Light availability and phytoplankton biomass were identified as the core drivers of PP, while WT, TOC, and nutrient dynamics exhibited context-dependent effects. Dual-scale buffer analysis revealed that PP variations were shaped not by isolated land use types but by their spatial configurations, where a balanced construction land-to-farmland ratio promoted PP levels, whereas excessive agricultural homogenization suppressed productivity. Additionally, ecologically sensitive basins displayed distinct PP regulation mechanisms, highlighting the importance of natural-agricultural synergies. These findings deepen our understanding of land use impacts on PP and provide a theoretical basis for optimizing land management strategies to balance eutrophication control with ecological productivity. Future research should further explore seasonal and hydrological influences to refine land use strategies for sustainable watershed management.

Conflict of interest

The authors declare that they have no known competing financial interests or personal relationships that could have appeared to influence the work reported in this study.

Acknowledgements

This study was jointly supported by the National Natural Science Foundation of China (42230513), the Key Program of the Shaanxi Key Laboratory of Environmental Monitoring and Forewarning of Trace Pollutants (SHJKFJJ 202307), and the Research Project on Ecological Protection and High-Quality Development in the Yellow River Basin, China (2022-YRUC-01-0101). We are grateful to the editor and the anonymous reviewers for providing helpful comments and suggestions.

Author contributions

Conceptualization: ZHANG Haoying, WANG Fei, TANG Bin, ZHANG Chaosong; Data analysis: ZHANG Haoying; Methodology: ZHANG Haoying, Guan Mengdan; Investigation: TANG Bin, ZHANG Chaosong, ZHANG Yuchen; Writing - original draft preparation: ZHANG Haoying, LI Nan; Written and edited: ZHANG Haoying, LI Nan; Financing acquisition: LI Nan, SONG Jinxi; Resources: ZHANG Haoying, TANG Bin, ZHANG Yuchen; Supervisor: LI Nan, SONG Jinxi; Visualization: ZHANG Haoying, GUAN Mengdan. All authors approved the manuscript.

References

Akinnawo S O. 2023. Eutrophication: Causes, consequences, physical, chemical and biological techniques for mitigation strategies. *Environmental Challenges*, 12: 100733, doi: 10.1016/j.envc.2023.100733.

Bai X L, Gu X H, Yang L Y. 2006. Analyses on water quality and its protection in east Lake Taihu. *Scientia Limnologica Sinica*, 18(1): 91–96. (in Chinese)

Bell C D, Tague C L, McMillan S K. 2019. Modeling runoff and nitrogen loads from a watershed at different levels of impervious surface coverage and connectivity to storm water control measures. *Water Resources Research*, 55(4): 2690–2707.

Bian G D, Wang G Q, Chen J, et al. 2021. Spatial and seasonal variations of hydrological responses to climate and land use changes in a highly urbanized basin of southeastern China. *Hydrology Research*, 52(2): 506–522.

Bonsdorff E. 2021. Eutrophication: early warning signals, ecosystem-level and societal responses, and ways forward. *Ambio*, 50: 753–758.

Booshaghi A S, Pachter L. 2021. Normalization of single-cell RNA-seq counts by $\log(x+1)$ or $\log(1+x)$. *Bioinformatics*, 37(15): 2223–2224.

Bratt A R, Finlay J C, Welter J R, et al. 2020. Co-limitation by N and P characterizes phytoplankton communities across nutrient availability and land use. *Ecosystems*, 23: 1121–1137.

Cadée G C. 1975. Primary production off the Guyana coast. *Netherlands Journal of Sea Research*, 9(1): 128–143.

Chang S, Wei Y Q, Dai Z Z, et al. 2024. Landscape ecological risk assessment and its driving factors in the Weihe River Basin, China. *Journal of Arid Land*, 16(5): 603–614.

Chinfak N, Sompongchaiyakul P, Charoenpong C, et al. 2023. Riverine and submarine groundwater nutrients fuel high primary production in a tropical bay. *Science of the Total Environment*, 877: 162896, doi: 10.1016/j.scitotenv.2023.162896.

Choi J, Min J O, Choi B, et al. 2020. Key factors controlling primary production and cyanobacterial harmful algal blooms (cHABs) in a continuous weir system in the Nakdong River, Korea. *Sustainability*, 12(15): 6224, doi: 10.3390/su12156224.

Cui G Y, Wang B L, Xiao J, et al. 2021. Water column stability driving the succession of phytoplankton functional groups in karst hydroelectric reservoirs. *Journal of Hydrology*, 592: 125607, doi: 10.1016/j.jhydrol.2020.125607.

Dokulil M T, Qian K M. 2021. Photosynthesis, carbon acquisition and primary productivity of phytoplankton: a review dedicated to Colin Reynolds. *Hydrobiologia*, 848: 77–94.

Doubek J P, Carey C C, Cardinale B J. 2015. Anthropogenic land use is associated with N-fixing cyanobacterial dominance in lakes across the continental United States. *Aquatic Sciences*, 77: 681–694.

Du J, Yang X, Xu P, et al. 2024. Linking water quality indicators in stable reservoir ecosystems: correlation analysis and ecohydrological implications. *Water*, 16(24): 3600, doi: 10.3390/w16243600.

Elser J J, Kyle M, Steger L, et al. 2009. Nutrient availability and phytoplankton nutrient limitation across a gradient of atmospheric nitrogen deposition. *Ecology*, 90(11): 3062–3073.

Fried S, Mackie B, Nothwehr E. 2003. Nitrate and phosphate levels positively affect the growth of algae species found in Perry Pond. *Tillers*, 4: 21–24.

Gove N E, Edwards R T, Conquest L L. 2001. Effects of scale on land use and water quality relationships: a longitudinal basin-wide perspective. *Journal of the American Water Resources Association*, 37(6): 1721–1734.

Haddout S, Priya K L, Hoguane A M, et al. 2022. Relationship of salinity, temperature, pH, and transparency to dissolved oxygen in the Bouregreg estuary (Morocco): First results. *Water Practice and Technology*, 17(12): 2654–2663.

Harmon L J, Glor R E. 2010. Poor statistical performance of the mantel test in phylogenetic comparative analyses. *Evolution*, 64(7): 2173–2178.

Harvey E T, Walve J, Andersson A, et al. 2019. The effect of optical properties on Secchi depth and implications for eutrophication management. *Frontiers in Marine Science*, 5: 496, doi: 10.3389/fmars.2018.00496.

Helsel D R, Hirsch R M, Ryberg K R, et al. 2020. Statistical methods in water resources. In: U.S. Geological Survey Techniques and Methods, Book 4, Chapter 8. Reston: U.S. Geological Survey, 210–219.

Huang P, Zhao X Q, Pu J W, et al. 2024. Defining the land use area threshold and optimizing its structure to improve supply-demand balance state of ecosystem services. *Journal of Geographical Sciences*, 34(5): 891–920.

Isles P D F, Creed I F, Jonsson A, et al. 2021. Trade-offs between light and nutrient availability across gradients of dissolved organic carbon lead to spatially and temporally variable responses of lake phytoplankton biomass to browning. *Ecosystems*, 24: 1837–1852.

Jia J J, Gao Y, Song X W, et al. 2019. Characteristics of phytoplankton community and water net primary productivity response to the nutrient status of the Poyang Lake and Gan River, China. *Ecohydrology*, 12(7): e2136, doi: 10.1002/eco.2136.

Kang J H, Huang H, Li W W, et al. 2018. Study of monthly variations in primary production and their relationships with environmental factors in the Daya Bay based on a general additive model. *Acta Oceanologica Sinica*, 37: 107–117.

Katsiapi M, Mazaris A D, Charalampous E, et al. 2012. Watershed land use types as drivers of freshwater phytoplankton structure. *Hydrobiologia*, 698: 121–131.

Knight C A. 2021. Causes and consequences of eutrophication, which are leading to water pollution. *Journal of Preventive Medicine*, 6(10): 118, doi: 10.36648/2572-5483.6.10.118.

Lee Y J, Ha S Y, Park H K, et al. 2015. Identification of key factors influencing primary productivity in two river-type reservoirs by using principal component regression analysis. *Environmental Monitoring and Assessment*, 187: 213, doi: 10.1007/s10661-015-4438-1.

Li B J, Song J X, Guan M C, et al. 2024. With spatial distribution, risk evaluation of heavy metals and microplastics to emphasize the composite mechanism in hyporheic sediments of Beiluo River. *Journal of Hazardous Materials*, 462: 132784, doi: 10.1016/j.jhazmat.2023.132784.

Li H H, Huang Y M, Guo W, et al. 2022. Influence of land use and land cover patterns on water quality at different spatio-temporal scales in Hehuang Valley. *Environmental Science*, 43(8): 4042–4053. (in Chinese)

Li X Y, Sun H L, Sun X L, et al. 2012. Temporal and spatial distribution of total organic carbon in Liusha Bay and the influence factors investigation. *Marine Sciences*, 36(7): 61–69. (in Chinese)

Liao J Q, Zhao L, Cao X F, et al. 2016. Cyanobacteria in lakes on Yungui Plateau, China are assembled via niche processes driven by water physicochemical property, lake morphology and watershed land-use. *Scientific Reports*, 6: 36357, doi: 10.1038/srep36357.

Liu E C, Lai Z N, Liu Q F, et al. 2022. The spatial-temporal variation characteristics and influencing factors of primary productivity in the mainstream of the Pearl River. *Chinese Fishery Quality and Standards*, 12(1): 12–21. (in Chinese)

Liu S S, Qiu Y, Fu R, et al. 2023. Identifying the water quality variation characteristics and their main driving factors from 2008 to 2020 in the Yellow River Basin, China. *Environmental Science and Pollution Research*, 30: 66753–66766.

Locke K A. 2024. Impacts of land use/land cover on water quality: A contemporary review for researchers and policymakers. *Water Quality Research Journal*, 59(2): 89–106.

Lü J Q, Zhang H H, Huang Y J, et al. 2024. Evolution characteristics and risk assessment on nonpoint source pollution in the Weihe River Basin, China. *Remote Sensing*, 16(23): 4605, doi: 10.3390/rs16234605.

Lu W Q, Zhang S Y, Zhou Z Z, et al. 2023. Effects of land use and physicochemical factors on phytoplankton community structure: The case of two fluvial lakes in the lower reach of the Yangtze River, China. *Global Ecology and Conservation*, 15(2): 180, doi: 10.3390/d15020180.

MacFarland T W, Yates J M. 2016. Introduction to Nonparametric Statistics for the Biological Sciences Using R. New York: Springer International Publishing, 249–297.

Ministry of Ecology and Environment of the People's Republic of China. 1990. Water Quality-Determination of Total Phosphorus-Ammonium Molybdate Spectrophotometric Method (GB11893-89). [2024-09-28]. https://www.mee.gov.cn/ywgz/fgbz/bz/bzwb/jcffbz/199007/t19900701_67131.shtml. (in Chinese)

Ministry of Ecology and Environment of the People's Republic of China. 2012. Water Quality-Determination of Total Nitrogen-Alkaline Potassium Persulfate Digestion UV Spectrophotometric Method (HJ 636-2012). [2024-09-16]. https://www.mee.gov.cn/ywgz/fgbz/bz/bzwb/jcffbz/201203/t20120307_224383.shtml. (in Chinese)

Miranda L E, Andrews C S, Kröger R. 2014. Connectedness of land use, nutrients, primary production, and fish assemblages in oxbow lakes. *Aquatic Sciences*, 76(1): 41–50.

Naipal V, Ciais P, Wang Y L, et al. 2018. Global soil organic carbon removal by water erosion under climate change and land use change during AD 1850–2005. *Biogeosciences*, 15(4): 4459–4480.

Oleksy I A, Solomon C T, Jones S E, et al. 2024. Controls on lake pelagic primary productivity: Formalizing the nutrient-color paradigm. *Journal of Geophysical Research: Biogeosciences*, 129(12): e2024JG008140, doi: 10.1029/2024JG008140.

Olson C R, Jones S E. 2022. Chlorophyll–total phosphorus relationships emerge from multiscale interactions from algae to catchments. *Limnology and Oceanography Letters*, 7(6): 483–491.

Parker A E, Dugdale R C, Wilkerson F P. 2012. Elevated ammonium concentrations from wastewater discharge depress primary productivity in the Sacramento River and the Northern San Francisco Estuary. *Marine Pollution Bulletin*, 64(3): 574–586.

Peng X, Zhang L, Li Y, et al. 2021. The changing characteristics of phytoplankton community and biomass in subtropical shallow lakes: Coupling effects of land use patterns and lake morphology. *Water Research*, 200: 117235, doi: 10.1016/j.watres.2021.117235.

Phileze P O. 2010. Variability of soil properties related to vegetation cover in a tropical rainforest landscape. *Journal of Geography and Regional Planning*, 3(7): 177–184.

Pilla R M, Griffiths N A. 2023. Integrating reservoirs into the dissolved organic matter versus primary production paradigm: How does chlorophyll-*a* change across dissolved organic carbon concentrations in reservoirs? *Ecosystems*, 27: 137–150.

Pramanik S. 2023. Assessment of spatial heterogeneity of landscape ecology of the Subarnarekha River Basin, India. *International Journal of Ecology and Environmental Sciences*, 49(5): 501, doi: 10.55863/ijees.v49i5.2813.

Preisner M, Neverova D E, Kowalewski Z. 2021. Mitigation of eutrophication caused by wastewater discharge: A simulation-based approach. *Ambio*, 50: 413–424.

Qu Y M, Wu N C, Guse B, et al. 2022. Distinct indicators of land use and hydrology characterize different aspects of riverine phytoplankton communities. *Science of the Total Environment*, 851: 158209, doi: 10.1016/j.scitotenv.2022.158209.

Quan J L, Xu Y X, Ma T, et al. 2022. Improving surface water quality of the Yellow River Basin due to anthropogenic changes. *Science of the Total Environment*, 836: 155607, doi: 10.1016/j.scitotenv.2022.155607.

Ren X F, Li P Y, He X D, et al. 2021. Hydrogeochemical processes affecting groundwater chemistry in the central part of the Guanzhong Basin, China. *Archives of Environmental Contamination and Toxicology*, 80: 74–91.

Sarkar S, Kumar S. 2024. Water stagnancy and wastewater input enhance primary productivity in an engineered river system. *River*, 3(2): 191–198.

Shiomoto A, Sasaki H, Nomura D. 2023. Size-fractionated phytoplankton biomass and primary production in the eastern Indian sector of the Southern Ocean in the austral summer 2018/2019. *Progress in Oceanography*, 218: 103119, doi: 10.1016/j.pocean.2023.103119.

Sinsomboonthong S. 2022. Performance comparison of new adjusted min-max with decimal scaling and statistical column normalization methods for artificial neural network classification. *International Journal of Mathematics and Mathematical Sciences*, 2022: 3584406, doi: 10.1155/2022/3584406.

Siqueira T D S, Pessoa L A, Vieira L, et al. 2023. Evaluating land use impacts on water quality: perspectives for watershed management. *Sustainable Water Resources Management*, 9(6): 192, doi: 10.1007/s40899-023-00968-2.

State Environmental Protection Administration of the People's Republic of China. 2002. *Water and Wastewater Monitoring and Analysis Method* (4th ed.). Beijing: China Environmental Science Press, 670–671. (in Chinese)

Sun J Z, Wang T F, Huang R P, et al. 2022. Enhancement of diatom growth and phytoplankton productivity with reduced O₂ availability is moderated by rising CO₂. *Communications Biology*, 5(1): 54, doi: 10.1038/s42003-022-03006-7.

Sun K, Deng W Q, Jia J J, et al. 2023. Spatiotemporal patterns and drivers of phytoplankton primary productivity in China's lakes and reservoirs at a national scale. *Global and Planetary Change*, 228: 104215, doi: 10.1016/j.gloplacha.2023.104215.

Tu J. 2011. Spatially varying relationships between land use and water quality across an urbanization gradient explored by geographically weighted regression. *Applied Geography*, 31(1): 376–392.

Wu J Y, Luo J G, Zhang H, et al. 2023. Driving forces behind the spatiotemporal heterogeneity of land-use and land-cover change: A case study of the Weihe River Basin, China. *Journal of Arid Land*, 15(3): 253–273.

Wu Q T, Li Y J, Shi X P, et al. 2022. Primary productivity assessment of typical reservoirs in Guangdong Province based on chlorophyll measurement. *Aquaculture*, 43(10): 4–8. (in Chinese)

Xie G H, Chen Y F, Zhou Y, et al. 2024. Steady-state transformation of phytoplankton community structure and its influencing factors in Honghu Lake. *Wetland Science*, 22(2): 264–272. (in Chinese)

Xu C, Jiang Y N, Su Z H, et al. 2022. Assessing the impacts of grain-for-green programme on ecosystem services in Jinghe River Basin, China. *Ecological Indicators*, 137: 108757, doi: 10.1016/j.ecolind.2022.108757.

Yamaguchi H, Koga N, Ichimi K, et al. 2020. Seasonal variations in phytoplankton productivity in a shallow cove in the eastern Seto Inland Sea, Japan. *Fisheries Science*, 86: 1067–1078.

Yan Z X, Li P, Li Z B, et al. 2023. Effects of land use and slope on water quality at multi-spatial scales: A case study of the Weihe River Basin. *Environmental Science and Pollution Research*, 30: 57599–57616.

Yang L Q, He X T, Ru S G, et al. 2024. Herbicide leakage into seawater impacts primary productivity and zooplankton globally. *Nature Communications*, 15(1): 1783, doi: 10.1038/s41467-024-46059-4.

Ye H B, Chen C Q, Sun Z H, et al. 2015. Estimation of the primary productivity in Pearl River estuary using MODIS data. *Estuaries and Coasts*, 38: 506–518.

Yu H F, Shi X H, Zhao S N, et al. 2022. Primary productivity of phytoplankton and its influencing factors in cold and arid regions: A case study of Wuliangsuhan Lake, China. *Ecological Indicators*, 144: 109545, doi: 10.1016/j.ecolind.2022.109545.

Zhang C, Li J, Zhou Z X, et al. 2021. Application of ecosystem service flows model in water security assessment: A case study in Weihe River Basin, China. *Ecological Indicators*, 120: 106974, doi: 10.1016/j.ecolind.2020.106974.

Zhang T, Su X L, Zhang G X, et al. 2022. Evaluation of the impacts of human activities on propagation from meteorological drought to hydrological drought in the Weihe River Basin, China. *Science of the Total Environment*, 819: 153030, doi: 10.1016/j.scitotenv.2022.153030.

Zhang X Q, Qi Y, Li H Y, et al. 2024. Assessing the response of non-point source nitrogen pollution to land use change based on SWAT model. *Ecological Indicators*, 158: 111391, doi: 10.1016/j.ecolind.2023.111391.

Zhao A Z, Zhu X F, Liu X F, et al. 2016. Impacts of land use change and climate variability on green and blue water resources in the Weihe River Basin of Northwest China. *CATENA*, 137: 318–327.

Zhao N, Zhang G L, Zhang S, et al. 2019. Temporal-spatial distribution of chlorophyll-*a* and impacts of environmental factors in the Bohai Sea and Yellow Sea. *IEEE Access*, 7: 160947–160960.

Zhao X Z, Li F M, Mo F, et al. 2012. Integrated conservation solutions for the endangered Loess Plateau of Northwest China. *Pakistan Journal of Botany*, 44: 77–83.

Zhong J, Wallin M B, Wang W F, et al. 2021. Synchronous evaporation and aquatic primary production in tropical river networks. *Water Research*, 200: 117272, doi: 10.1016/j.watres.2021.117272.

Zuo D P, Bi Y Q, Song Y H, et al. 2023. The response of non-point source pollution to land use change and risk assessment based on model simulation and grey water footprint theory in an agricultural river basin of Yangtze River, China. *Ecological Indicators*, 154: 110581, doi: 10.1029/2024JG008.

Appendix

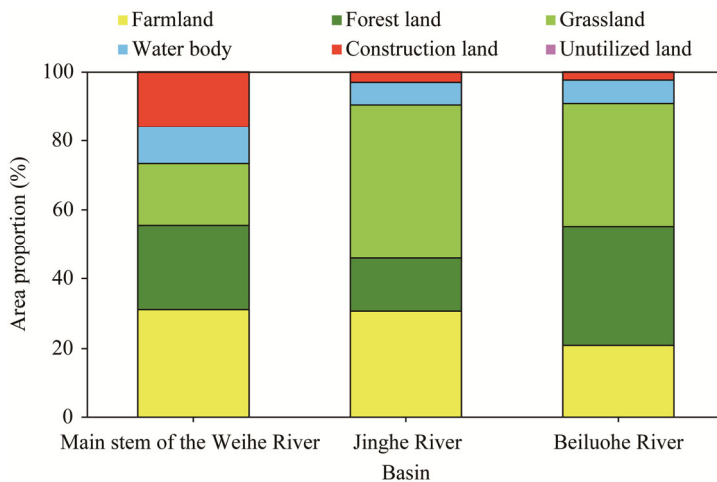


Fig. S1 Area proportion of each land use type in the Weihe River Basin

Table S1 Physical-chemical property of water of each river in the Weihe River Basin

River	SUN (h/d)	SD (m)	pH	WT (°C)	DO (mg/L)	TOC (mg/L)	TN (mg/L)	TP (mg/L)	TN/TP ratio
Main stem of the Weihe River	13.16± 0.13	0.19± 0.22	8.47± 0.31	17.33± 4.89	9.487± 1.078	30.238± 38.763	5.562± 1.463	0.457± 0.768	608.997± 920.026
	13.77± 0.15	0.14± 0.13	8.38± 0.13	18.60± 2.89	9.156± 0.929	14.034± 7.486	3.863± 1.877	0.014± 0.015	1028.504± 1529.976
Jinghe River	14.19± 0.03	0.37± 0.25	8.68± 0.16	21.70± 3.89	10.674± 1.360	9.549± 1.760	8.094± 6.606	0.013± 0.004	713.902± 766.634

Note: Mean±SD. SUN, sunlight duration; SD, Secchi depth; WT, water temperature; DO, dissolved oxygen; TOC, total organic carbon; TN, total nitrogen; TP, total phosphorus; TN/TP ratio, ratio of total nitrogen to total phosphorus.